Golovynskyi et al. Nanoscale Research Letters (2018) 13:103
https://doi.org/10.1186/s11671-018-2524-3

Nanoscale Research Letters

NANO EXPRESS Open Access

Interband Photoconductivity of Metamorphic InAs/InGaAs Quantum Dots in the 1.3–1.55-μm Window

Sergii Golovynskyi[1,2], Oleksandr I. Datsenko[3], Luca Seravalli[4], Giovanna Trevisi[4], Paola Frigeri[4], Ivan S. Babichuk[1,2], Iuliia Golovynska[1] and Junle Qu[1*]

Abstract

Photoelectric properties of the metamorphic InAs/$In_xGa_{1-x}As$ quantum dot (QD) nanostructures were studied at room temperature, employing photoconductivity (PC) and photoluminescence spectroscopies, electrical measurements, and theoretical modeling. Four samples with different stoichiometry of $In_xGa_{1-x}As$ cladding layer have been grown: indium content x was 0.15, 0.24, 0.28, and 0.31. InAs/$In_{0.15}Ga_{0.85}As$ QD structure was found to be photosensitive in the telecom range at 1.3 μm. As x increases, a redshift was observed for all the samples, the structure with $x = 0.31$ was found to be sensitive near 1.55 μm, i.e., at the third telecommunication window. Simultaneously, only a slight decrease in the QD PC was recorded for increasing x, thus confirming a good photoresponse comparable with the one of $In_{0.15}Ga_{0.75}As$ structures and of GaAs-based QD nanostructures. Also, the PC reduction correlate with the similar reduction of photoluminescence intensity. By simulating theoretically the quantum energy system and carrier localization in QDs, we gained insight into the PC mechanism and were able to suggest reasons for the photocurrent reduction, by associating them with peculiar behavior of defects in such a type of structures. All this implies that metamorphic QDs with a high x are valid structures for optoelectronic infrared light-sensitive devices.

Keywords: Nanostructure, Quantum dot, Metamorphic, InAs/InGaAs, Photoconductivity, Photoluminescence, Photocurrent

Background

Metamorphic InAs/$In_xGa_{1-x}As$ QD nanostructures have attracted much interest in the last decade owing to many benefits [1–7]. Their most attractive feature is that, by growing the QDs on an InGaAs metamorphic buffer (MB), one can achieve a significant reduction of the transition energy between the QD levels [8] with respect to conventional In(Ga)As/GaAs QD structures. This occurs due to the decrease of InAs QD bandgap as a result of the lattice mismatch reduction between InAs QDs and InGaAs buffer and, hence, the strain in QDs [9–11]. So, the application of a MB as a confining material allows to shift the emission wavelength value deeper into the infrared (IR) range, in particular, into the telecommunication windows at 1.3 and 1.55 μm, while maintaining a high efficiency [4, 12, 13]. Furthermore, metamorphic QDs have shown interesting properties such as (i) a high QD density [14], (ii) the possibility to widely tune QD and wetting layer (WL) levels [10, 15], and (iii) good performances of active elements in light-emitting devices [16]. However, the recent investigations of deep levels in metamorphic QDs showed that, despite InAs/$In_{0.15}Ga_{0.85}As$ QD structures having a total defect density close to the QD layer comparable to that of InGaAs/GaAs pseudomorphic QDs, metamorphic structures with higher x demonstrated higher defect densities [17, 18].

Metamorphic InAs QD structures have found successful applications in the design and fabrication of IR photonic and light-sensitive devices, such as lasers [19, 20], single-photon sources [3, 7, 21, 22], and solar cells [23–25]. In(Ga)As QD photodetectors based on interband and intersubband transitions are currently actively investigated for enhanced detection from near-IR to longwave-IR

* Correspondence: jlqu@szu.edu.cn
[1]Key Laboratory of Optoelectronic Devices and Systems of Ministry of Education and Guangdong Province, College of Optoelectronic Engineering, Shenzhen University, Shenzhen 518060, People's Republic of China
Full list of author information is available at the end of the article

ranges due to their response to the irradiation at normal incidence [26–30]. For instance, the intersubband transitions of electrons between quantum-confined levels and continuum states can be engineered by embedding InAs QDs in InGaAs layers [29–32], as this design allows to tune the detection peak wavelength, to control the response by an externally applied bias and to reduce the dark current [33, 34]. To date, there are no papers about the implementation of metamorphic QD structures in photodetectors.

The key role for the development of this area is the preservation of a high emission efficiency and photosensitivity of metamorphic QD structures that need to be at least comparable with those of conventional InAs/GaAs QD structures [1, 5, 35]. A lot of studies were carried out in the fundamental and application fields to develop structure design [6, 14, 21], to improve photoelectric properties [5, 13], and to control/reduce strain-related defects in the heterostructures [4, 36, 37].

Hence, InAs/$In_xGa_{1-x}As$ metamorphic QD nanostructures are interesting nanostructures, which allow to have emission or photoresponsivity in the 1.3- and 1.55-μm IR ranges [1–7]. Furthermore, it was reported by us earlier that vertical InAs/$In_{0.15}Ga_{0.75}As$ QD structures can maintain photosensitivity comparable to the GaAs-based ones [5]. However, such metamorphic structures are seldom studied in photoelectric measurements with a lateral geometry, where the photocurrent proceeds through in-plane transport of carriers across channels between two top contacts. Commonly, the QD layers along with the associated WL form these conductivity channels in the lateral geometry-designed GaAs-based structures [38]. Owing to this peculiar type of conductivity, QD photodetectors with the lateral transport are believed to have potential for a high photoresponsivity [39, 40]. An in-depth study of metamorphic InAs/InGaAs QD nanostructures in the lateral configuration can provide a fundamental knowledge about the photoconductivity (PC) mechanism and efficiency of the in-plain carrier transport. In our recent paper devoted to the defects in metamorphic QD structures [17], we reported lateral PC measurements at low temperatures, considering only the IR spectra edges originating from defects. However, we believe that a proper characterization and fundamental investigation of the structure at room temperature can give precious insights for further improvements of novel light-sensitive devices as near-IR photodetectors, linear arrays, and camera matrixes, by implementing metamorphic QDs.

In the present work, we studied in-plane photoelectric properties of the metamorphic InAs/$In_xGa_{1-x}As$ QD nanostructures grown by molecular beam epitaxy with different In composition x, employing PC and photoluminescence (PL) spectroscopies, lateral electrical measurements, and modeling calculations. In particular, we focused on the observation of a possible redshift of the QD layer photoresponse toward the IR beyond 1.3 μm while preserving photosensitivity alike for $In_{0.15}Ga_{0.85}As$ and GaAs QD light-sensitive structures. A high photosensitivity in the near-IR wavelength range at room temperature is an indication that these nanostructures can be useful not only for devices based on interband transitions but also for intersubband photodetectors working beyond 10 μm.

Methods

Sample Preparation and Description

The studied structures schematically shown in Fig. 1 were grown by molecular beam epitaxy. Firstly, a semi-insulating (100) GaAs substrate was covered by a 100-nm thick GaAs buffer at 600 °C, followed by the deposition of an undoped InGaAs MB 500 nm in thickness at 490 °C. Then, after the prior growth interruption of 210 s to cool down the substrate, 3.0 MLs (monolayers) of InAs were grown at 460 °C. Finally, these self-assembled QDs were covered by 20 nm of undoped $In_xGa_{1-x}As$ with the same MB stoichiometry. Four samples with different stoichiometry of $In_xGa_{1-x}As$ cladding layer have been fabricated: In content x was 0.15, 0.24, 0.28, and 0.31.

Theoretical Modeling

For metamorphic structure designing as well as understanding of the energy profile, the calculations of the quantum energy system composed by In(Ga)As QDs, undoped MB, and cap layer were carried out by using the Tibercad software [41] that we demonstrated to be

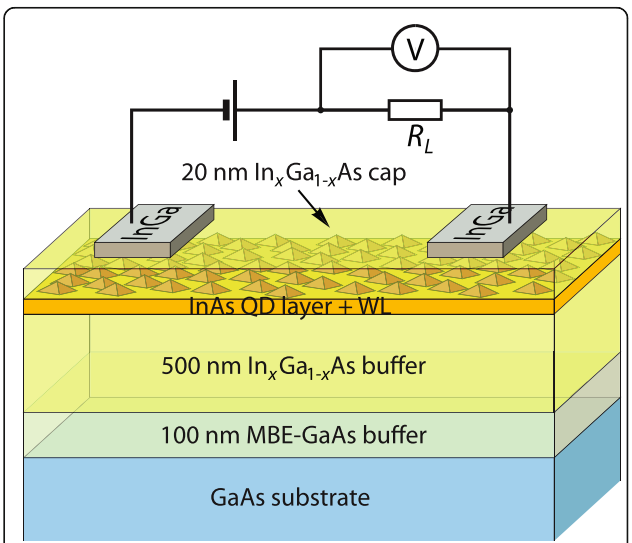

Fig. 1 Color online. Scheme of the metamorphic InAs/$In_xGa_{1-x}As$ QD structures and their connection for the photoelectric measurements

adequate to simulate the optical properties of semiconductor low-dimensional nanostructures [2, 15, 42].

We consider an InAs QD with truncated conical shape and sizes taken from experimental atomic force microscopy data [14]; we include the presence of InAs WL, which parameters depend on the $In_xGa_{1-x}As$ metamorphic layer properties [15].

First, strain calculations for the structure are made, by calculating the strain tensor components of the QD, induced by the mismatch f_{QD} between the QD and MB, defined as

$$f_{QD} = [a_{InAs} - a_{MB}(x)]/a_{MB}(x) \quad (1)$$

where $a_{MB}(x)$ is the lattice parameter of $In_xGa_{1-x}As$ MB and a_{InAs} is the lattice parameter of InAs. Then, band profiles for QDs and embedding layers depend on the deformation potentials of the relevant materials (InAs for QDs and WLs and relaxed InGaAs for MB).

Finally, the Schrödinger equation

$$\boldsymbol{H}\psi = E\psi \quad (2)$$

is solved in the envelope function approximation by a single-band, effective-mass approach for electrons and 6 bands k•p approach for holes, where the 3D Hamiltonian is

$$\hat{H} = -\frac{\eta^2}{2}\nabla_{\mathbf{r}}\left(\frac{1}{m(E,\mathbf{r})}\right)\nabla_{\mathbf{r}} + V(\mathbf{r}), \quad (3)$$

with $V(\mathbf{r})$ being the 3D potential.

Such an approximation is considered satisfying when carrying on QD ground state calculation [2]. Ground levels for electrons and heavy holes are thus obtained, alongside their probability densities. Photoluminescence emission energies were derived by taking the energy difference between confined levels for electrons and heavy holes, reduced by 20 meV to take into consideration excitonic effects.

A more detailed description of model calculations can be found in Ref. [2].

Photoelectric Characterization

For the lateral photoelectric measurements, two InGa eutectic surface contacts were deposited over 5 × 2 mm pieces of the structures. Measured linear *I*–*V* characteristics given in Fig. 2 have confirmed the contact ohmicity. The current flowing through the samples was measured by a Siglent SDM3055 multimeter, using a standard dc technique [43, 44] as a voltage drop across a series load resistance R_L of 1 MΩ, which was much less than the sample resistance. Photocurrent was excited by a 250-W halogen lamp light dispersed with a prism monochromer, and PC spectra were recorded in the range from 0.6 to 1.6 eV [44–46]. The spectra were normalized to the excitation quanta number of the light source. PL spectra were obtained using a 532-nm laser as an excitation source with a power density of 5 W/cm^2. All the measurements were carried out at room temperature (300 K).

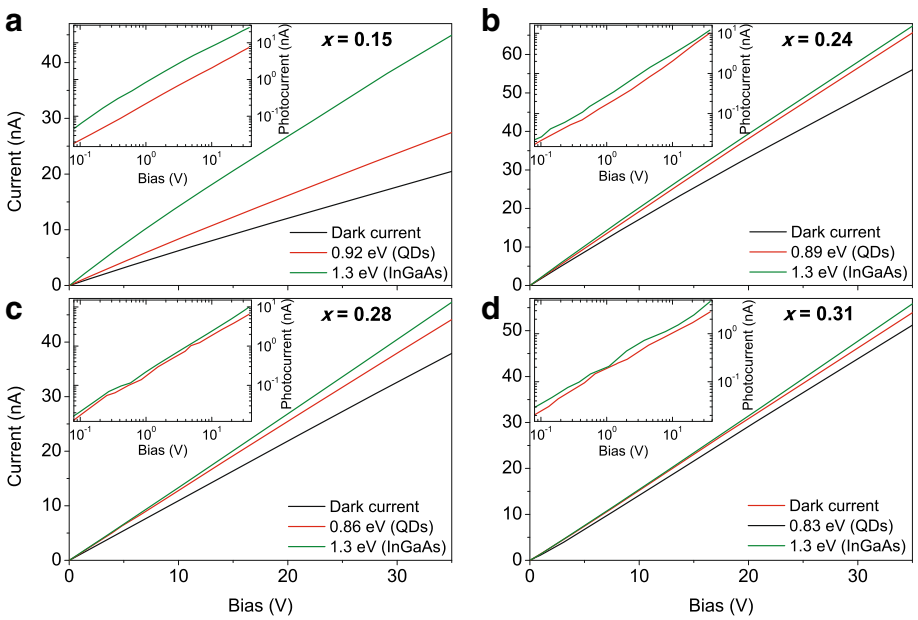

Fig. 2 Color online. *I*–*V* characteristics of the InAs/$In_xGa_{1-x}As$ structures with $x = 0.15$ (**a**), 0.24 (**b**), 0.28 (**c**), and 0.31 (**d**) for the dark (black) and under an illumination of 350 μW/cm^2 (color) at energies of PL spectrum peak (QD excitation) and 1.3 eV (effective absorption in InGaAs). Insets: photocurrent dependences on bias voltage

Results and Discussion

PC spectra of the studied metamorphic InAs/$In_xGa_{1-x}As$ QD structures at room temperature are given in Fig. 3 together with the PL bands, which show the optical transitions between QD ground states. The relative intensities and positions of the PL bands are also shown in Fig. 4b. Features due to the QDs, InGaAs confining layers, and GaAs bottom layers are observed on the PC curves. The photocurrent signal at the energies below the PL band onsets could be related to the structure defects detected earlier [17].

The investigated metamorphic InAs/$In_{0.15}Ga_{0.85}As$ QD structure was found to be photosensitive in the telecom range at 0.95 eV (1.3 μm) (Fig. 3a). As x increased, a redshift was observed for all the samples: the structure with $x = 0.31$ was found to be sensitive near 0.8 eV (1.55 μm) (Fig. 3d), i.e., at the third telecom window [47]. The shift is related to the reduction of the lattice mismatch between the materials of InAs QD and $In_xGa_{1-x}As$ buffer with an increase in x and, hence, a decrease in the strain in QDs. This leads to a narrowing of the InAs QD bandgap and, in turn, to the redshift of the PL band as well as the photoresponse onset toward IR [1–6, 19, 35].

Simultaneously, only a slight decrease in the QD photocurrent signal was recorded, thus confirming the preservation of a good photoresponsivity, comparable with that of the $In_{0.15}Ga_{0.75}As$ sample. As we discussed recently [5], metamorphic QD structures with $x = 0.15$ show a photoresponse very similar to those of pseudomorphic InAs/GaAs QD nanostructures. Also, the PC reduction correlate with the PL one as it can be seen in Fig. 3.

Such an effect for our samples turned out to be most notable in Fig. 2, where the I–V dependences at the dark and under illumination at different characteristic spectral points on bias voltage are shown, together with the photocurrent dependences in the insets. Like in Fig. 3, the photocurrent value implies just the photoinduced part of current obtained from the total current under illumination by subtracting the dark current value. These spectral points are the PL band maximums and 1.3 eV, where an effective band-to-band absorption in InGaAs MB occurs. As well as for the dark I–V characteristics, these dependencies are linear-like within the experimental error.

The best photoresponse was measured in the structure with the minimal In content in the confining layers. It also had the lowest dark current. The photocurrent value at the applied excitation level (350 μW/cm^2) in the InAs/$In_{0.15}Ga_{0.85}As$ structure was two to three times above the dark current when MB was pumped. The photoresponse at QD excitation was comparable to the dark current; however, it should be considered that our structures had only one QD layer. Fabrication of the multilayered QD structures surely would lead to a significant increase in the IR photoresponse. Other

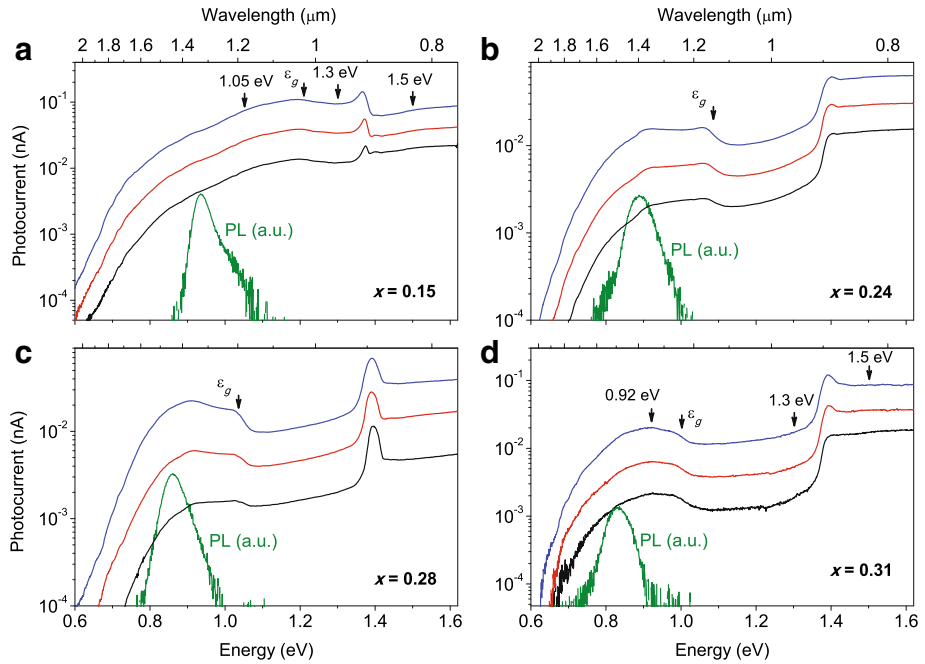

Fig. 3 Color online. PC spectra of the metamorphic InAs/$In_xGa_{1-x}As$ structures at room temperature and a bias of 11 V for $x = 0.15$ (**a**), 0.24 (**b**), 0.28 (**c**), and 0.31 (**d**). The excitation intensities for the black, red, and blue curves at 1.3 eV correspond to 88, 350, and 1400 μW/cm^2, respectively. PL spectra in arbitrary units are given for the energy positioning of QD ground state transitions. The vertical arrows mark the InGaAs bandgaps (ε_g) calculated following Paul et al. [48] and spectral positons, where the PC dependencies on excitation intensity were measured (given in Fig. 5)

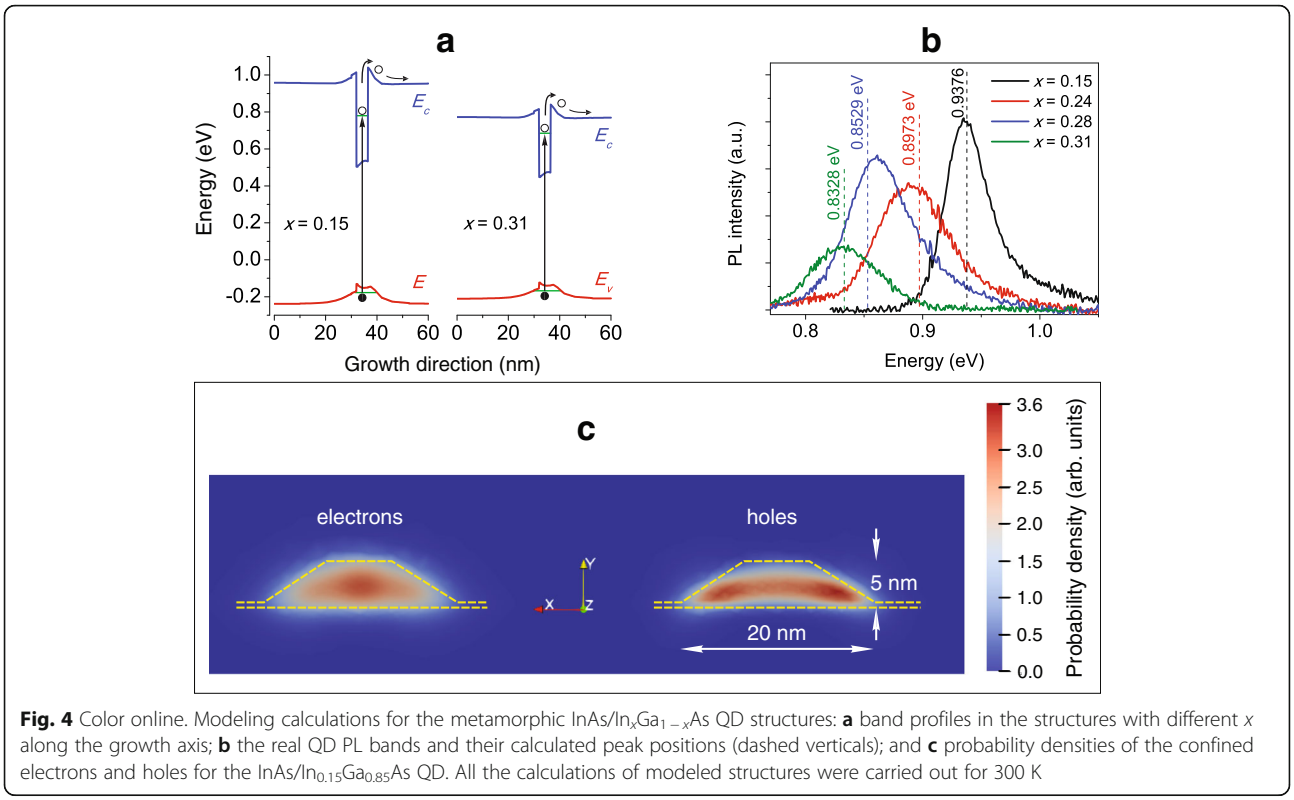

Fig. 4 Color online. Modeling calculations for the metamorphic InAs/$In_xGa_{1-x}As$ QD structures: **a** band profiles in the structures with different *x* along the growth axis; **b** the real QD PL bands and their calculated peak positions (dashed verticals); and **c** probability densities of the confined electrons and holes for the InAs/$In_{0.15}Ga_{0.85}As$ QD. All the calculations of modeled structures were carried out for 300 K

structures with higher *x* revealed lower photocurrent signals; the detected magnitudes at both spectral points were approximately an order lower than the dark current values in a wide range of the applied voltage. The lowest photoresponse was found for the InAs/$In_{0.31}Ga_{0.69}As$ structure with the maximal MB In content.

Most probably, this photoresponsivity decrease is related to an increase in the MB defect density with *x*, which was determined earlier for these structures, employing deep level thermally stimulated current spectroscopy [17], that correlated well with structural analysis of such nanostructures [1]. We have reported that the InAs/$In_{0.15}Ga_{0.85}As$ QD structure had a total defect density close to the QD layer comparable to InGaAs/GaAs ones, whereas other structures with higher In contents demonstrated higher densities of defects like the known GaAs-related point defect complexes EL2, EL6, EL7, EL9, and EL10 near the QD layer and three levels attributed to extended defects propagating through the buffer.

In regard to the spectrum shape (Fig. 3), above the QD excitation, light absorption and, hence, the carrier generation occur mainly in the MB at energies above the InGaAs confining layer bandgap ε_g, which values for different *x* were estimated by an empiric formula [48]. However, it is noteworthy that an increase in photon energy above ε_g leads to a slight decrease of the photoresponse. Naturally, this confirms that metamorphic QDs, despite being effective recombination centers [1, 2, 12, 22], are more efficient contributors to photocurrent than MB [5, 6, 23].

To understand the PC mechanism of this peculiarity, one should look at Fig. 4a, where we show the calculated QD band profiles along the growth direction for our samples. Calculations are validated by the result of quantum energy levels for electrons and holes: the expected PL emission energies are in agreement with the PL QD ground state transition measured experimentally (Fig. 4b). In Fig. 4c, we show the simulated probability densities for confined electrons and holes, obtained by the carrier wavefunctions calculated with the Tibercad modelization, that indicate a higher level of localization for heavy holes in comparison with electrons.

In order to contribute to the photocurrent signal, electron-hole pairs generated by QD interband absorption have to escape from QDs by thermal emission. In a previous study [49], it was established that in metamorphic QDs electrons and heavy holes escape simultaneously from QDs as correlated pairs. Moreover, it was also demonstrated that the activation energy for such process corresponds to the sum of the activation energies for the two particles [50].

While studying thermal quenching of PL emission from metamorphic QDs [10, 51], we proved that such activation energies are equal to the sum of the energy distance from the WL levels and QD states and go from

250 meV for $x = 0.15$ down to 150 meV for $x = 0.31$. As widely discussed in Ref. [51], these values cause a strong quenching of the PL emission at room temperature via the thermal escape of confined carriers.

On such basis, we can infer that carriers excited in QDs can thermally escape to WL and MB: there, electrons and heavy holes are separated by the band bending in the QD vicinity (Fig. 4a), which promotes the hole trapping back to QDs and, while being a barrier for electrons, thereby effectively suppresses their radiative recombination. As a consequence, heavy holes are concentrated at the QD periphery (Fig. 4c), whereas electrons are free to move along the potential well of WL and MB contributing to the conductivity. It is worth noting that in Ref. [49], it is discussed that, although correlated during the escape process, carriers cannot be considered as excitons at room temperature; henceforth, they can be easily separated by the band bending in the vicinity of QDs.

Otherwise, when exciting the MB, non-equilibrium holes are generated in the confining layers and do recombine with electrons. It should be mentioned here that the WL is known to be a conductivity channel for nanostructures based on GaAs [52] and, in our lateral structures designed with surface contacts, there is no heterojunction, so carriers are efficiently collected near the surface plane.

In Fig. 3, the fall of PC signal just above ε_g turned into the rise at higher energies, e.g., above 1.3 or 1.1 eV for sample with x of 0.15 or 0.31, respectively. This was conceivably caused by the optical absorption closer to the surface and QD layer, thus involving shallower traps. As established for these structures by thermally stimulated current spectroscopy and deep level transient spectroscopy [17, 18], the deeper electron traps are located mainly in the InGaAs MB layer, whereas the shallower ones are concentrated near the surface (in relation to these samples, near the QD layer). The electrons trapped into the shallower traps can more easily escape back to the conduction band at room temperature. Thus, free electrons near the QD layer are more mobile than those excited deeper in the MB and, hence, give a higher contribution to the charge transfer. Furthermore, the electrons, being generated near the surface, can freely transfer to the WL conductivity channel.

A similar drop of photocurrent following an increase above GaAs bandgap (near 1.4 eV) was observed. This effect might be due to the carrier generation close to the InGaAs/GaAs interface, which is known to have a higher density of defect states being traps and recombination centers.

The relative contribution of different optical transitions to the structure photoresponse varied with pumping intensity. This is better observed in Fig. 5, which shows photocurrent values as a function of the excitation intensity at different characteristic spectral points: the onset of the PL band (resonant excitation of the QD ensemble) or efficient band-to-band absorption in InGaAs (1.3 eV) and GaAs (1.5 eV).

The structures with different In contents in the confining layers demonstrated similar dependencies at equivalent spectral ranges. So, the band-to-band excitation in GaAs (1.5 eV) shows a quadratic dependence at most of intensity values. This is typical for the band-to-band recombination of non-equilibrium charge carriers, for instance when they are highly predominant under the equilibrium carriers [53]: this is expectable in our undoped structures. The dependencies in the case of excitation in the QD and InGaAs confining layers are very similar to each other but different from those for GaAs. They are linear at low excitation intensities and become sublinear at higher intensities. This behavior obviously points out to the carrier recombination involving Shockley-Read centers: the linear dependence becomes sublinear one, as some of the centers are saturated at higher carrier generation rates [54]. These results of intensity-dependent measurements distinctly indicate an efficient generation of main charge carriers at a relatively

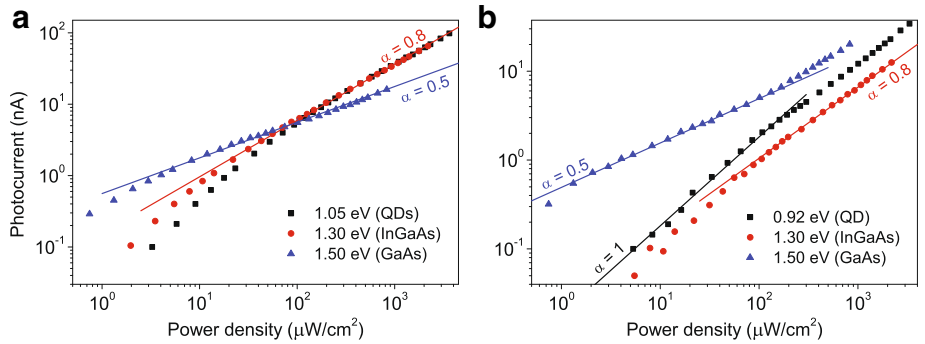

Fig. 5 Color online. Photocurrent vs excitation intensity for the InAs/$In_xGa_{1-x}As$ structures with **a** $x = 0.15$ and **b** 0.31. The lines are the fitting by functions $f(x) \sim x^{\alpha}$

low recombination rate in QD embedding layers and a much higher density of recombination centers in GaAs layers. For example, during the QD excitation in similar characterizations, InGaAs/GaAs QD photosensitive structures showed a dependence from intensity as $PC(I) \sim I^{0.25}$, which occurred due to a high rate of the non-radiative recombination though defect levels along with QD radiative recombination [40, 55]. However, it is worth to notice that the InGaAs/GaAs structure was multilayered having seven QD layers.

From these measurements and their interpretation, some indications for the use of metamorphic QDs for IR detection can be highlighted: (i) when using $x > 0.15$, advanced designs allowing to control strain-related defects should be used, similar to what was done for the development of metamorphic QDs [19, 20, 37]; (ii) multilayer stacks of QDs (with a minimum of 10 layers) are needed to obtain a QD PC above the dark current [27, 56]; and (iii) as a higher confinements of heavy holes is beneficial for the photocurrent obtained when exciting QDs, advanced designs with higher-gap barriers for heavy holes could be considered [51, 57]. Hence, these findings can be very useful for the design of metamorphic QDs aiming at IR detection and the development of metamorphic QD photodetectors.

Conclusions

Photoelectric properties of the metamorphic InAs/$In_xGa_{1-x}As$ QD nanostructures were studied at room temperature, employing PC and PL spectroscopies, electrical measurements, and theoretical model simulations. The studied metamorphic InAs/$In_xGa_{1-x}As$ QD nanostructures were found to be photosensitive in the telecommunication windows at 1.3 ($x = 0.15$) and 1.55 μm ($x = 0.31$). However, the QD PC as well as the PL efficiencies of the structures with higher In contents in MB were estimated to be lower and, nevertheless, comparable to that of the InAs/$In_{0.15}Ga_{0.85}As$ structure, which has sensitivity similar to InGaAs/GaAs QD structures. This photoresponsivity reduction is related to an increase in the MB defect density with x. Also, thanks to modeling calculations, we provided insights into the PC mechanism in the investigated type of QD structures. All this implies that metamorphic QDs with a high x are valid structures for optoelectronic IR light-sensitive devices, provided that some points of concern are addressed by optimization of the design of the nanostructure.

Abbreviations

ε_g: Bandgap of the InGaAs confining layer; E_c and E_v: Energy of conductivity and valence bands; IR: Infrared; MB: Metamorphic buffer; ML: Monolayer; PC: Photoconductivity; PL: Photoluminescence; QD: Quantum dot; R_L: The load resistance; WL: Wetting layer

Funding

This work was supported in part by COST Action "Nanoscale Quantum Optics" of European Union; National Natural Science Foundation of China (61525503, 61620106016, 81727804); National Basic Research Program of China (2015CB352005); Guangdong Natural Science Foundation Innovation Team (2014A030312008); Shenzhen Basic Research Project (JCYJ20150930104948169, JCYJ20160328144746940, GJHZ20160226202139185, JCYJ20170412105003520); and Ministry of Education and Science of Ukraine.

Availability of Data and Materials

All data are fully available without restriction.

Authors' Contributions

SG, OD, and LS proposed and guided the overall project. LS, GT, and PF designed and grew the samples, measured the luminescence spectra, and carried out the calculations. SG and OD made the electrical contacts and technical part. SG, OD, ISB, and IG performed the photoelectrical measurements. SG, OD, and LS wrote the manuscript, with contributions from all authors. JQ participated in the discussions and edited the manuscript. LS and JQ provided managerial supports, supervising the research. All authors reviewed and approved the final manuscript.

Authors' Information

SG (Ph.D.), ISB (Ph.D.), IG (Ph.D.), and JQ (professor) are from Key Laboratory of Optoelectronic Devices and Systems of Ministry of Education and Guangdong Province, College of Optoelectronic Engineering, Shenzhen University, Shenzhen 518060, People's Republic of China. SG and ISB are visiting researchers in the Institute of Semiconductor Physics, National Academy of Sciences, Kyiv 03028, Ukraine. OD (Ph.D.) is from the Department of Physics, Taras Shevchenko National University of Kyiv, Kyiv 01601, Ukraine. LS (Ph.D.), GT (Ph.D.), and PF (Ph.D.) are from the Institute of Materials for Electronics and Magnetism, CNR-IMEM, 43100 Parma, Italy.

Competing Interests

The authors declare that they have no competing interests.

Publisher's Note

Author details

[1]Key Laboratory of Optoelectronic Devices and Systems of Ministry of Education and Guangdong Province, College of Optoelectronic Engineering, Shenzhen University, Shenzhen 518060, People's Republic of China. [2]Institute of Semiconductor Physics, NAS of Ukraine, Kyiv 03028, Ukraine. [3]Department of Physics, Taras Shevchenko National University of Kyiv, Kyiv 01601, Ukraine. [4]Institute of Materials for Electronics and Magnetism, CNR-IMEM, I-43124 Parma, Italy.

Received: 28 December 2017 Accepted: 10 April 2018
Published online: 16 April 2018

References

1. Seravalli L, Frigeri P, Nasi L, Trevisi G, Bocchi C (2010) Metamorphic quantum dots: quite different nanostructures. J Appl Phys 108:064324
2. Gioannini M, Cedola AP, Di Santo N, Bertazzi F, Cappelluti F (2013) Simulation of quantum dot solar cells including carrier intersubband dynamics and transport. IEEE J Photovoltaics 3:1271
3. Munoz-Matutano G, Barrera D, Fernandez-Pousa CR, Chulia-Jordan R, Seravalli L, Trevisi G et al (2016) All-optical fiber Hanbury Brown & Twiss interferometer to study 1300 nm single photon emission of a metamorphic InAs quantum dot. Sci Rep 6:27214
4. Semenova ES, Zhukov AE, Mikhrin SS, Egorov AY, Odnoblyudov VA, Vasil'ev AP et al (2004) Metamorphic growth for application in long-wavelength (1.3-1.55 μm) lasers and MODFET-type structures on GaAs substrates. Nanotechnology 15:S283–S2S7
5. Golovynskyi S, Seravalli L, Datsenko O, Trevisi G, Frigeri P, Gombia E et al (2017) Comparative study of photoelectric properties of metamorphic InAs/InGaAs and InAs/GaAs quantum dot structures. Nanoscale Res Lett 12:335
6. Golovynskyi S, Seravalli L, Datsenko O, Kozak O, Kondratenko SV, Trevisi G et al (2017) Bipolar effects in photovoltage of metamorphic InAs/InGaAs/

GaAs quantum dot heterostructures: characterization and design solutions for light-sensitive devices. Nanoscale Res Lett 12:559
7. Paul M, Olbrich F, Höschele J, Schreier S, Kettler J, Portalupi SL et al (2017) Single-photon emission at 1.55 μm from MOVPE-grown InAs quantum dots on InGaAs/GaAs metamorphic buffers. Appl Phys Lett 111:033102
8. Trevisi G, Seravalli L, Frigeri P, Prezioso M, Rimada JC, Gombia E et al (2009) The effects of quantum dot coverage in InAs/(In)GaAs nanostructures for long wavelength emission. Microelectron J 40:465–468
9. Seravalli L, Minelli M, Frigeri P, Allegri P, Avanzini V, Franchi S (2003) The effect of strain on tuning of light emission energy of InAs/InGaAs quantum dot nanostructures. Appl Phys Lett 82:2341–2343
10. Seravalli L, Minelli M, Frigeri P, Franchi S, Guizzetti G, Patrini M et al (2007) Quantum dot strain engineering of InAs/InGaAs nanostructures. J Appl Phys 101:024313
11. Wang P, Chen QM, Wu XY, Cao CF, Wang SM, Gong Q (2016) Detailed study of the influence of InGaAs matrix on the strain reduction in the InAs dot-in-well structure. Nanoscale Res Lett 11:119
12. Seravalli L, Frigeri P, Trevisi G, Franchi S (2008) 1.59 μm room temperature emission from metamorphic InAs/InGaAs quantum dots grown on GaAs substrates. Appl Phys Lett 92:213104
13. Golovynskyi SL, Seravalli L, Trevisi G, Frigeri P, Gombia E, Dacenko OI et al (2015) Photoelectric properties of the metamorphic InAs/InGaAs quantum dot structure at room temperature. J Appl Phys 117:214312
14. Seravalli L, Trevisi G, Frigeri P (2012) 2D-3D growth transition in metamorphic InAs/InGaAs quantum dots. CrystEngComm 14:1155–1160
15. Seravalli L, Trevisi G, Frigeri P (2013) Calculation of metamorphic two-dimensional quantum energy system: application to wetting layer states in InAs/InGaAs metamorphic quantum dot nanostructures. J Appl Phys 114:184309
16. Mi Z, Wu C, Yang J, Bhattacharya P (2008) Molecular beam epitaxial growth and characteristics of 1.52 μm metamorphic InAs quantum dot lasers on GaAs. J Vac Sci Technol 26:1153
17. Golovynskyi S, Datsenko O, Seravalli L, Kozak O, Trevisi G, Frigeri P et al (2017) Deep levels in metamorphic InAs/InGaAs quantum dot structures with different composition of the embedding layers. Semicond Sci Technol 32:125001
18. Rimada JC, Prezioso M, Nasi L, Gombia E, Mosca R, Trevisi G et al (2009) Electrical and structural characterization of InAs/InGaAs quantum dot structures on GaAs. Mater Sci Eng B-Adv 165:111–114
19. Mi Z, Bhattacharya P (2008) Pseudomorphic and metamorphic quantum dot heterostructures for long-wavelength lasers on GaAs and Si (invited paper). IEEE J Sel Top Quant 14:1171–1179
20. Karachinsky LY, Kettler T, Novikov II, Shernyakov YM, Gordeev NY, Maximov MV et al (2006) Metamorphic 1.5 μm-range quantum dot lasers on a GaAs substrate. Semicond Sci Technol 21:691–696
21. Seravalli L, Trevisi G, Frigeri P (2012) Design and growth of metamorphic InAs/InGaAs quantum dots for single photon emission in the telecom window. CrystEngComm 14:6833–6838
22. Seravalli L, Trevisi G, Frigeri P, Rivas D, Munoz-Matutano G, Suarez I et al (2011) Single quantum dot emission at telecom wavelengths from metamorphic InAs/InGaAs nanostructures grown on GaAs substrates. Appl Phys Lett 98:173112
23. Azeza B, Alouane MHH, Ilahi B, Patriarche G, Sfaxi L, Fouzri A et al (2015) Towards InAs/InGaAs/GaAs quantum dot solar cells directly grown on Si substrate. Materials 8:4544–4552
24. Rouis W, Haggui M, Rekaya S, Sfaxi L, M'ghaieth R, Maaref H et al (2016) Local photocurrent mapping of InAs/InGaAs/GaPts intermediate-band solar cells using scanning near-field optical microscopy. Sol Energ Mat Sol C 144: 324–330
25. Han IS, Kim JS, Kim JO, Noh SK, Lee SJ (2016) Fabrication and characterization of InAs/InGaAs sub-monolayer quantum dot solar cell with dot-in-a-well structure. Curr Appl Phys 16:587–592
26. Wu J, Chen SM, Seeds A, Liu HY (2015) Quantum dot optoelectronic devices: lasers, photodetectors and solar cells. J Phys D Appl Phys 48:363001
27. Passmore BS, Jiang W, Manasreh MO, Kunets VP, Lytvyn PM, Salamo GJ (2008) Room temperature near-infrared photoresponse based on interband transitions in $In_{0.35}Ga_{0.65}As$ multiple quantum dot photodetector. IEEE Electron Device Lett 29:224–227
28. Kondratenko SV, Iliash SA, Vakulenko OV, Mazur YI, Benamara M, Marega E et al (2017) Photoconductivity relaxation mechanisms of InGaAs/GaAs quantum dot chain structures. Nanoscale Res Lett 12:183
29. Shao J, Vandervelde TE, Barve A, Stintz A, Krishna S (2012) Increased normal incidence photocurrent in quantum dot infrared photodetectors. Appl Phys Lett 101:241114
30. Vaillancourt J, Stintz A, Meisner MJ, Lu XJ (2009) Low-bias, high-temperature operation of an InAs-InGaAs quantum-dot infrared photodetector with peak-detection wavelength of 11.7 μm. Infrared Phys Technol 52:22–24
31. Lu X, Meisner MJ, Vaillancourt J, Li J, Liu W, Qian X, Goodhue WD (2007) Modulation-doped InAs-InGaAs quantum dot longwave infrared photodetector with high quantum efficiency. Electron Lett 43:589–590
32. Lu XJ, Vaillancourt J, Meisner MJ, Stintz A (2007) Long wave infrared InAs-InGaAs quantum-dot infrared photodetector with high operating temperature over 170K. J Phys D Appl Phys 40:5878–5882
33. Lin W-H, Chao K-P, Tseng C-C, Mai S-C, Lin S-Y, Wu M-C (2009) The influence of In composition on InGaAs-capped InAs/GaAs quantum-dot infrared photodetectors. J Appl Phys 106:054512
34. Nedzinskas R, Čechavičius B, Rimkus A, Pozingytė E, Kavaliauskas J, Valušis G et al (2015) Temperature-dependent modulated reflectance of InAs/InGaAs/GaAs quantum dots-in-a-well infrared photodetectors. J Appl Phys 117:144304
35. Seravalli L, Frigeri P, Minelli M, Franchi S, Allegri P, Avanzini V (2006) Metamorphic self-assembled quantum dot nanostructures. Mat Sci Eng C-Bio S 26:731–734
36. Mi Z, Bhattacharya P, Yang J (2006) Growth and characteristics of ultralow threshold 1.45 μm metamorphic InAs tunnel injection quantum dot lasers on GaAs. Appl Phys Lett 89:153109
37. Mazzucato S, Nardin D, Capizzi M, Polimeni A, Frova A, Seravalli L et al (2005) Defect passivation in strain engineered InAs/(InGa)As quantum dots. Mat Sci Eng C-Bio S 25:830–834
38. Kunets Vas P, Rebello Sousa Dias M, Rembert T, Ware ME, Mazur Yu I, Lopez-Richard V et al (2013) Electron transport in quantum dot chains: dimensionality effects and hopping conductance. J Appl Phys 113:183709
39. Towe E, Pan D (2000) Semiconductor quantum-dot nanostructures: their application in a new class of infrared photodetectors. J Sel Top Quantum Electron 6:408
40. Golovynskyi SL, Dacenko OI, Kondratenko SV, Lavoryk SR, Mazur YI, Wang ZM et al (2016) Intensity-dependent nonlinearity of the lateral photoconductivity in InGaAs/GaAs dot-chain structures. J Appl Phys 119:184303
41. Auf der Maur M, Penazzi G, Romano G, Sacconi F, Pecchia A, Di Carlo A (2011) The multiscale paradigm in electronic device simulation. IEEE Trans Electron Devices 58:1425–1432
42. Trevisi G, Seravalli L, Frigeri P (2016) Photoluminescence monitoring of oxide formation and surface state passivation on InAs quantum dots exposed to water vapor. Nano Res 9:3018–3026
43. Kondratenko SV, Vakulenko OV, Mazur YI, Dorogan VG, Marega E, Benamara M et al (2014) Deep level centers and their role in photoconductivity transients of InGaAs/GaAs quantum dot chains. J Appl Phys 116:193707
44. Vakulenko OV, Golovynskyi SL, Kondratenko SV (2011) Effect of carrier capture by deep levels on lateral photoconductivity of InGaAs/GaAs quantum dot structures. J Appl Phys 110:043717
45. Kondratenko SV, Golovinskiy SL, Vakulenko OV, Kozyrev YN, Rubezhanska MY, Vodyanitsky AI (2007) Photocurrent spectroscopy of indirect transitions in Ge/Si multilayer quantum dots at room temperature. Surf Sci 601:L45–LL8
46. Valakh MY, Dzhagan VM, Yukhymchuk VO, Vakulenko OV, Kondratenko SV, Nikolenko AS (2007) Optical and photoelectrical properties of GeSi nanoislands. Semicond Sci Technol 22:326–329
47. Song H-Z, Hadi M, Zheng Y, Shen B, Zhang L, Ren Z et al (2017) InGaAsP/InP nanocavity for single-photon source at 1.55-μm telecommunication band. Nanoscale Res Lett 12:128
48. Paul S, Roy JB, Basu PK (1991) Empirical expressions for the alloy composition and temperature-dependence of the bandbap and intrinsic carrier density in $Ga_xIn_{1-x}As$. J Appl Phys 69:827–829
49. Sanguinetti S, Colombo D, Guzzi M, Grilli E, Gurioli M, Seravalli L et al (2006) Carrier thermodynamics in $InAs/In_xGa_{1-x}As$ quantum dots. Phys Rev B 74:205302
50. Le Ru EC, Fack J, Murray R (2003) Temperature and excitation density dependence of the photoluminescence from annealed InAs/GaAs quantum dots. Phys Rev B 67:1–12
51. Seravalli L, Trevisi G, Frigeri P, Franchi S, Geddo M, Guizzetti G (2009) The role of wetting layer states on the emission efficiency of InAs/InGaAs metamorphic quantum dot nanostructures. Nanotechnology 20:275703

52. Danil'tsev VM, Drozdov MN, Moldavskaya LD, Shashkin VI, Germanenko AV, Min'kov GM et al (2004) Electron transport effects in the IR photoconductivity of InGaAs/GaAs structures with quantum dots. Tech Phys Lett 30:795–798
53. Sze SM, Ng KK (2006) Physics of semiconductor devices. Wiley-Interscience, New Jersey
54. Duboc CA (1955) Nonlinearity in photoconducting phosphors. Br J Appl Phys 6:107–111
55. Golovynskyi SL, Mazur YI, Wang ZM, Ware ME, Vakulenko OV, Tarasov GG et al (2014) Excitation intensity dependence of lateral photocurrent in InGaAs/GaAs dot-chain structures. Phys Lett A 378:2622–2626
56. Ezzedini M, Hidouri T, Alouane MHH, Sayari A, Shalaan E, Chauvin N et al (2017) Detecting spatially localized exciton in self-organized InAs/InGaAs quantum dot superlattices: a way to improve the photovoltaic efficiency. Nanoscale Res Lett 12:450
57. Seravalli L, Frigeri P, Allegri P, Avanzini V, Franchi S (2007) Metamorphic quantum dot nanostructures for long wavelength operation with enhanced emission efficiency. Mater Sci Eng C 27:1046–1051